The use of quad–quad resistivity in helicopter electromagnetic mapping

Haoping Huang* and Douglas C. Fraser‡

ABSTRACT

The apparent resistivity from a helicopter-borne frequency-domain electromagnetic (EM) system is typically obtained from the in-phase and quadrature responses arising from the flow of conduction currents in the earth. The most commonly used resistivity algorithms, derived from half-space models and using single-frequency data, do not account for magnetic polarization and consequently do not yield a reliable value for apparent resistivity in highly magnetic areas. This is because magnetic polarization modifies the EM response, causing the computed resistivity to be erroneously high. The impact of magnetic permeability on the EM response is much greater for the in-phase component than for the quadrature component. If magnetic polarization is to be ignored, the calculation of the apparent resistivity using the quadrature component at two frequencies (the quad–quad algorithm) is less subject to error from magnetic polarization than if the in-phase and quadrature responses at a single frequency are used (the in-phase–quad algorithm). The quad–quad algorithm, however, can display undesirable behavior for large induction numbers, i.e., when conductivities and frequencies are large. Determining which algorithm is optimum is a data-dependent choice, which, of course, is area dependent.

We have studied the behavior of the quad–quad (apparent) resistivity and its comparison to in-phase–quad resistivity to determine the conditions under which the use of quad–quad resistivity is appropriate. For a two-layer earth, the behavior of the quad–quad resistivity depends mainly upon the ratio of the lower frequency f_L to the upper-layer resistivity ρ_1. If this ratio is low, the quad–quad resistivity will behave well. In areas yielding a high value of the ratio f_L/ρ_1, the quad–quad resistivity may lie outside of the range of the true resistivities of the earth and therefore provide misleading information. Our studies therefore suggest that the quad–quad resistivity algorithm should be avoided in areas where the ratio is large, i.e., when using high frequencies in conductive areas. The term large is relative. For a two-layer case, for example, the use of quad–quad resistivity is only recommended for magnetic areas where $f_L/\rho_1 < 500$ Hz/ohm-m, when conductive cover exists, and where $f_L/\rho_1 < 50$ Hz/ohm-m when a conductive basement underlies resistive cover. In spite of these limitations, quad–quad resistivity is often preferable to in-phase–quad resistivity in highly magnetic areas.

INTRODUCTION

Huang and Fraser (2000) discuss the use of the quadrature responses from two adjacent frequencies of a helicopter-borne electromagnetic (EM) system to compute the apparent resistivity of the earth. This contrasts with the usual method of computing the apparent resistivity from the in-phase and quadrature response from a single frequency using techniques developed by Fraser (1978). We refer to the apparent resistivity obtained from two quadrature responses as quad–quad resis-

tivity, in contrast to the in-phase–quad resistivity computed from a single frequency. In this paper, we assume the reader is familiar with the contents of Huang and Fraser (2000), where the quad-quad technique is introduced. We now investigate further the behavior of dual-frequency quad–quad resistivity, comparing it to single-frequency in-phase–quad resistivity.

The apparent resistivity for a given EM sensor array can be defined in a number of ways (Spies and Eggers, 1986). In particular, there are at least 14 definitions of apparent resistivity for frequency-domain helicopter EM systems (Figure 1, Table 1).

It may be helpful to place our study in the context of these definitions.

Fraser (1990) provides five different definitions or transforms (Table 1, 1–5) for the apparent resistivity from half-space models based on helicopter EM input parameters from a single frequency. Of these five half-space transforms, the pseudolayer half-space transform 1 of Figure 1b is preferred for displaying the apparent resistivity in both plan (e.g., Fraser, 1978) and

section (e.g., Sengpiel, 1988). It has two advantages over the other four half-space transforms (2–5), all of which use the homogeneous half-space model of Figure 1a. First, the pseudolayer half-space model and its transform 1 do not use flight height as an input; therefore, the apparent resistivity is immune to sensor–source distance errors caused by the altimeter's response to forests and rugged topography. Second, its sensitivity to resistivity variations at depth is significantly greater

Table 1. Fourteen half-space resistivity transforms characterized by their input parameters. The parameters I, Q, A, and ϕ refer, respectively, to the input in-phase, quadrature, EM amplitude $(I^2 + Q^2)^{1/2}$, and phase ratio Q/I for a given frequency; Q_L and Q_H refer to the quadrature response for a lower and a higher frequency, respectively. For magnetic conductive half-space transforms (6, 7, 14), the magnetic permeability μ is first determined from the lowest frequency and then applied as input for each of the higher frequencies. For dielectric conductive half-space transforms (8–11), with or without magnetic permeability, the dielectric permittivity ε is first determined from the highest frequency and then applied as input for the lower frequencies if necessary. The output resistivity and sensor–source distance are respectively indicated by ρ and h (Figure 1).

| Transform	Input	Output	No. of freqs	Half-space model	Use in practice
Applicable for nonpermeable, nondielectric half-spaces					
1	I, Q (or A, ϕ)	ρ, h	1	Pseudolayer	Most common use
2	A, a	ρ	1	Homogeneous	Use has diminished
3	ϕ, a	ρ	1	Homogeneous	Not used
4	I, a	ρ	1	Homogeneous	Not used
5	Q, a	ρ	1	Homogeneous	Not used
Applicable for permeable half-spaces					
6	I, Q, μ	ρ, h	1	Pseudolayer	Limited use
7	A, a, μ	ρ	1	Homogeneous	Not used
Applicable for dielectric half-spaces					
8	I, Q, ε	ρ, h	1	Pseudolayer	Limited use
9	A, a, ε	ρ	1	Homogeneous	Not used
Applicable for permeable dielectric half-spaces					
10	I, Q, μ, ε	ρ, h	1	Pseudolayer	Limited use
11	A, a, μ, ε	ρ	1	Homogeneous	Not used
Applicable for nonpermeable and permeable half-spaces					
12	Q_L, Q_H	ρ, h	2	Pseudolayer	Subject of this paper
13	Q_L, Q_H, a	ρ	2	Homogeneous	Subject of this paper
14	Q_L, Q_H, μ	ρ, h	2	Pseudolayer	Subject of this paper
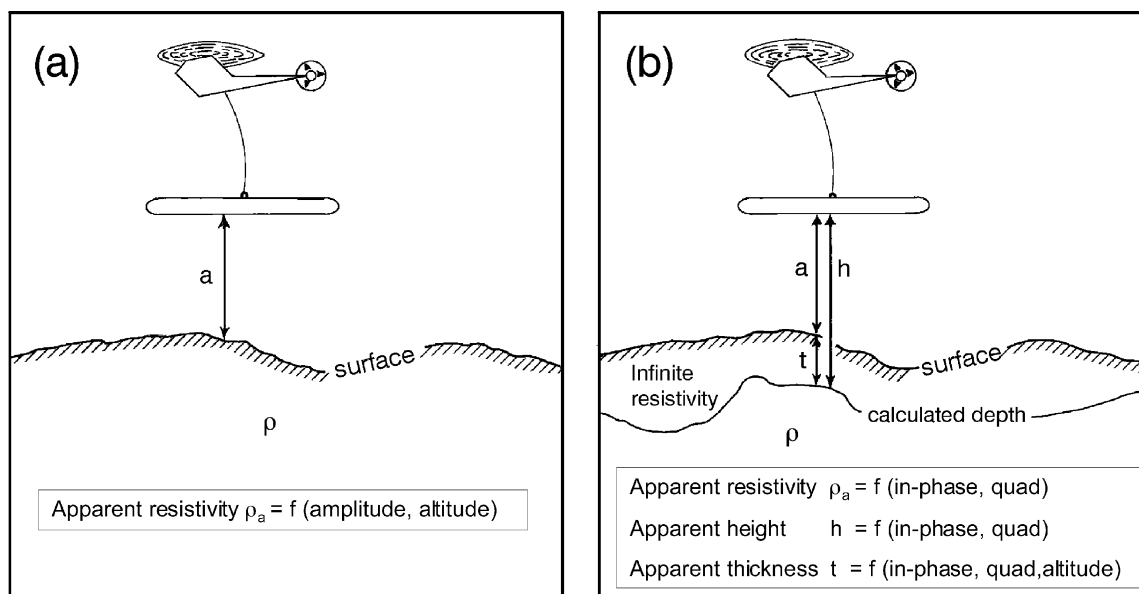
FIG. 1. (a) The homogeneous half-space model, where the top of the half-space coincides with the earth's surface as defined by the radar or laser altimeter. Amplitude refers to the square root of the sum of the squares of the in-phase and quadrature components. (b) The pseudolayer half-space model, where the top of the half-space is defined numerically by the output parameter h. The pseudolayer half-space model is equivalent to a two-layer case where the upper layer is of infinite resistivity. The thickness t of the pseudolayer is the difference between the computed height h and the measured bird altitude a as obtained from the altimeter. The argument list for the function f may change in accordance with the Input column of Table 1.

than for the homogeneous half-space model, as will be seen below.

When the EM data are impacted by magnetic permeability or dielectric permittivity, transforms 1–5 of Table 1 can yield misleading apparent resistivities; for such situations, the resistivity transforms 6–11 of Table 1 are applicable (Huang and Fraser, 2000, 2001, 2002). These transforms require the correct permeability and/or permittivity to yield the correct apparent resistivity.

Huang and Fraser (2000) describe additional apparent resistivity transforms defined by the quadrature responses from any two, usually adjacent, frequencies. One such transform is shown as 12 of Table 1. It is of interest because it yields an apparent resistivity that is fairly independent of magnetic permeability. However, magnetic permeability can be an input variable when computing quad–quad resistivity, as shown in transform 14 of Table 1, although it generally has little impact on the computed resistivity.

The quad–quad technique, while of value in magnetic terrain for computing resistivity, has not been thoroughly presented, and so a user could be unaware of its potential problems. Our paper shows that quad–quad resistivity sometimes exhibits undesirable behavior. For example, the apparent resistivity values may fall above (overshoot) or below (undershoot) the range of the true resistivities of the materials present in a layered earth. Overshoots and undershoots are artifacts of the resistivity computation and have been reported elsewhere for other EM techniques (e.g., Morrison et al., 1969). These issues are important because the behavior of an apparent resistivity parameter limits the usefulness of interpretation techniques based on apparent resistivity as input, e.g., the use of a differential resistivity (Huang and Fraser, 1996; Sengpiel and Siemon, 2000).

In the synthetic examples shown below, the forward solutions are obtained from equation (1) in Huang and Fraser (2000) through Hankel transformation. The sensor–source distance (flying height) is taken as 30 m, which is common for helicopter EM surveys. For a homogeneous earth, the apparent resistivity computed from EM data using any half-space algorithm is independent of flying height and matches the true resistivity. However, for a layered earth, the apparent resistivity is a slowly varying function of flying height. For example, a 1000-Hz helicopter EM system flown over a two-layer earth (10-m-thick upper layer of 10 ohm-m and a lower layer of 100 ohm-m) will yield in-phase–quad resistivities of 39.5 and 42.1 ohm-m, respectively, for flying heights of 30 and 40 m when using transform 1. This paper does not further discuss the impact of flying height variations.

APPARENT RESISTIVITY ALGORITHMS

Apparent resistivity is traditionally defined as the resistivity of a homogeneous half-space that will produce the same response as measured over the real earth with the same geophysical system. All system arrays and all half-space models and algorithms yield the true resistivity when the earth is a true homogeneous half-space, but all tend to yield different apparent resistivities when the earth is inhomogeneous, e.g., layered.

Single-frequency algorithms

The apparent resistivity ρ_a and apparent height h_a of the pseudolayer model of Figure 1b (transforms 1 and 6, Table 1)

can be written as functions of the in-phase I and quadrature Q responses at a single frequency and an optional relative magnetic permeability μ_r, i.e.,

$$\{\rho_a, h_a\} = f(I, Q, \mu_r). \quad (1)$$

The apparent thickness of the pseudolayer at that frequency is obtained from

$$t_a = h_a - a, \quad (2)$$

where a is the EM bird altitude determined from the altimeter.

For the homogeneous half-space model of Figure 1a, the apparent resistivity can be written for a single frequency and an optional relative magnetic permeability μ_r as

$$\rho_a = f(I, Q, a, \mu_r), \quad (3)$$

where I and Q may be taken separately (transforms 4, 5) or, more usually, may be taken in combination to yield a single input parameter, typically the EM amplitude $A = (I^2 + Q^2)^{1/2}$ (transforms 2 and 7).

Figure 2 shows the normalized apparent resistivity as a function of the normalized skin depth, obtained from the in-phase–quad algorithms of the pseudolayer and homogeneous half-space models, for a suite of nonmagnetic two-layer cases for the helicopter EM system. The apparent resistivity of Figure 2a, derived from the pseudolayer half-space model (transform 1), is more sensitive to the lower layer (i.e., the underlying half-space) than the apparent resistivity of Figure 2b from the homogeneous half-space model (transform 2). This is evident because the apparent resistivity from the pseudolayer model has a greater dynamic range at medium values of the abscissa than that from the homogeneous half-space model, especially when the lower layer is conductive. Also, the amount of overshoot and undershoot in the apparent resistivity (when the abscissa is approximately 1) is larger for the homogeneous half-space model than for the pseudolayer half-space model. For these reasons, the pseudolayer half-space model is preferred for in-phase–quad resistivity.

Dual-frequency algorithms

Huang and Fraser (2000) define an apparent resistivity based on a pseudolayer half-space model similar to Figure 1b, using the quadrature responses at two frequencies. The in-phase component is ignored. The quadrature responses Q_L and Q_H from a lower frequency f_L and an adjacent higher frequency f_H, respectively, are used to compute an apparent resistivity ρ_a and an apparent height h_a. The apparent resistivity and height can be written as

$$\{\rho_a, h_a\} = f(Q_L, Q_H, \mu_r), \quad (4)$$

where μ_r is an optional input relative magnetic permeability (cf. transforms 12 and 14). As for the single-frequency in-phase–quad algorithm, the apparent thickness of the pseudolayer of Figure 1b for the two-frequency quad–quad algorithm is obtained from equation (2).

The quad–quad apparent resistivity can also be computed from variants of the homogeneous half-space model of Figure 1a, i.e.,

$$\rho_a = f(Q_L, Q_H, a, \mu_r), \quad (5)$$

where a is the sensor–source distance. The low- and high-frequency quadrature responses Q_L and Q_H are combined to yield a single input parameter, typically the ratio Q_L/Q_H or an amplitude function such as $(Q_L + Q_H)$ or $(Q_L^2 + Q_H^2)^{1/2}$. The homogeneous half-space model yields two solutions to the apparent resistivity when using either of these quadrature amplitude functions. However, the solution is unique when using the quadrature ratio. Hence, we deal only with the quadrature ratio when computing the quad–quad resistivity using the homogeneous half-space model, e.g., transform 13 in which the magnetic permeability is ignored.

Figure 3 shows the apparent resistivity curves, obtained from the quad–quad algorithms of the pseudolayer and homogeneous half-space models, for a suite of nonmagnetic two-layer cases for the helicopter EM system. The apparent resistivities of Figure 3a, obtained from the pseudolayer half-space model [equation (4)], and Figure 3b, from the homogeneous half-space model [equation (5)], have roughly equal sensitivity to the resistivity of the lower layer. However, the resistivity from the homogeneous half-space model exhibits large overshoot for the conductive upper-layer case at high values of the abscissa of Figure 3b. For example, note the upper curve of this figure. The ordinate ratio saturates at the correct value of 1000 for high values of the abscissa, but prior to saturation the ordinate ratio overshoots to 10 000. This means the apparent resistivity exceeds the true resistivity of the most resistive layer by a factor of 10. Thus, as for the in-phase–quad algorithms, the pseudolayer half-space model yields superior results to the
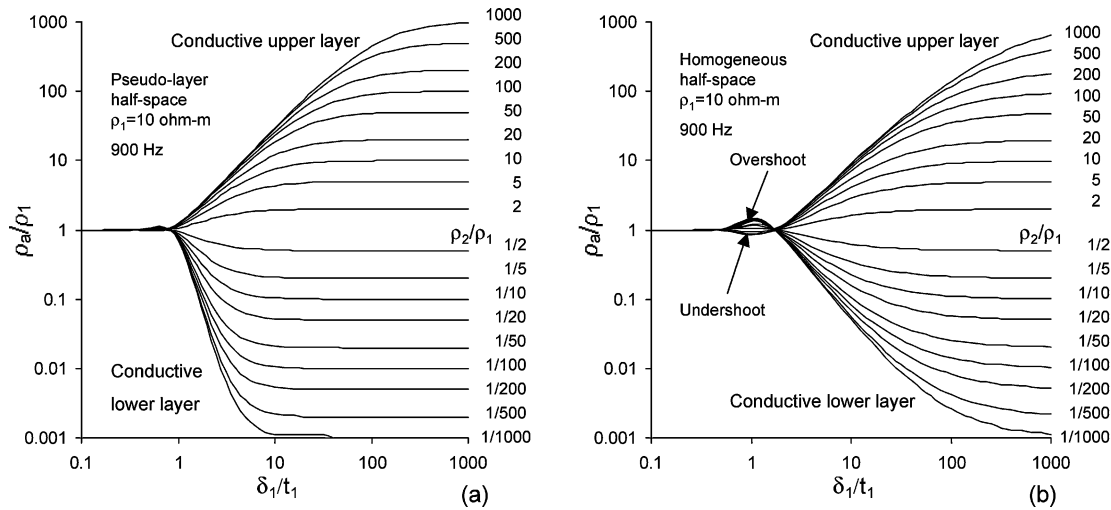

FIG. 2. A comparison of normalized in-phase–quad resistivity curves for a suite of two-layer cases for (a) the pseudolayer half-space model using transform 1 of Table 1 and (b) the homogeneous half-space model using transform 2. The ratio of the lower-layer resistivity ρ_2 to the upper-layer resistivity ρ_1 varies from 1/1000 to 1000 for these 18 cases. The abscissa represents the skin depth δ_1 of the upper layer normalized against its thickness t_1. The ordinate is the computed apparent resistivity ρ_a normalized against the resistivity ρ_1 of the upper layer. (The curves are specific for a flying height a (Figure 1) of 30 m and for the ratio $f/\rho_1 = 90$ Hz/ohm-m, where f is the frequency, equating to a skin depth in the upper layer of 53 m.)
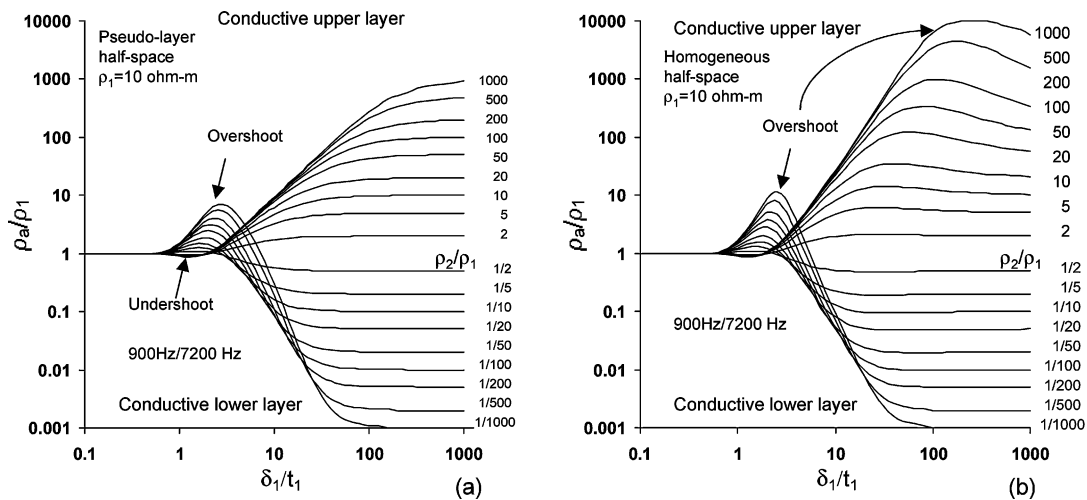

FIG. 3. A comparison of the quad–quad resistivity curves for a suite of two-layer cases for (a) the pseudolayer half-space model using transform 12 and (b) the homogeneous half-space model using transform 13. See Figure 2 for the abscissa and ordinate. (The curves are specific for the ratio $f_L/\rho_1 = 90$ Hz/ohm-m, where f_L is the low frequency of the pair, equating to a skin depth in the upper layer of 53 m for this frequency.)

homogeneous half-space model for the quad–quad resistivity. Consequently, the homogeneous half-space model will not be considered further.

We now compare the apparent resistivity curves obtained from quad–quad transform 12 of Figure 3a with those from in-phase–quad transform 1 of Figure 2a. Both sets of curves are from the pseudolayer model for the same suite of two-layer cases. The quad–quad algorithm (Figure 3a) has less sensitivity to the resistivity of the lower layer (at midabscissa value) than the in-phase–quad algorithm (Figure 2a), and it exhibits a more serious overshoot (at low abscissa value), although it has little undershoot. With these deficiencies, there needs to be a good reason to use the quad–quad algorithm in preference to the in-phase–quad algorithm for computing the resistivity. This reason lies with reducing the effect of magnetic permeability on the response of the input EM parameters.

QUAD–QUAD APPARENT RESISTIVITY

The following examples deal only with the pseudolayer resistivity model, using both the in-phase–quad and quad–quad algorithms. The quad–quad resistivity technique was originally proposed for use in magnetic areas that are also resistive (Huang and Fraser, 1998). In such areas, conduction currents are minimal and magnetic polarization currents may dominate. Magnetic permeability has a much lesser impact on the quadrature component than on the in-phase component. Thus, the quad–quad resistivity of transform 12 is less affected by magnetic permeability than the in-phase–quad resistivity of transform 1. Also, the quad–quad resistivity may be less affected by errors in the calculated magnetic permeability than the in-phase–quad resistivity of transform 6. We use synthetic two-layer data to test the quad–quad method and compare it to the in-phase–quad method. A number of layered earths with various combinations of resistivities, thicknesses, and permeabilities have been studied. Representative cases are presented below using frequencies and frequency ratios characteristic of most Dighem helicopter-borne EM systems.

Nonmagnetic two-layer cases

Since the quad–quad method is a new analytic technique, for simplicity we focus first on the behavior of quad–quad resistivity for nonmagnetic cases. Then we discuss the effect of magnetization on quad–quad resistivity and compare it to in-phase–quad resistivity.

The behavior of quad–quad resistivity can be undesirable under certain circumstances. For example, when resistivity is low or frequencies are high, significant overshoot and undershoot in the computed resistivity may occur. Figure 4a shows the 900/7200 Hz quad–quad resistivity for two-layer cases where the resistivities of the upper layer vary from 1 to 500 ohm-m and ρ_2/ρ_1 is fixed at 1/50. The amount of the resistivity overshoot of the ordinate ρ_a/ρ_1 of Figure 4a for these conductive basement cases increases with decreasing values of the upper-layer resistivity ρ_1. The maximum resistivity overshoot occurs at values of the abscissa δ_1/t_1 in the range of 1.5 to 3, depending on the upper-layer resistivity. The quad–quad resistivity overshoot can yield apparent resistivities that are 10 times higher than the upper-layer resistivity, which itself is higher than the resistivity of the lower conductive layer or half-space. This means the overshoot can yield apparent resistivities that lie outside the range of the true resistivities of the two-layer model by as much as a factor of 10 for this particular series of two-layer cases. In contrast to these quad–quad resistivity results, the in-phase–quad resistivity curves of Figure 4b exhibit only negligible overshoot for these two-layer cases.

The amount of apparent resistivity overshoot and undershoot increases with the frequencies used to compute the quad–quad resistivity. Figure 5a presents 7200/56 000 Hz quad–quad resistivity for two two-layer cases. The upper-layer resistivity is 10 ohm-m, and the resistivity contrasts ρ_2/ρ_1 are 1/50 and 50. The apparent resistivity overshoots by a factor of 10 for the conductive lower-layer case. In Figure 4a, where the ratio of high to low frequency is also about 8 but the frequencies are lower (i.e., 900/7200 Hz), the apparent resistivity overshoots by a factor of only 2.2 for the same case of $\rho_1 = 10$ ohm-m.
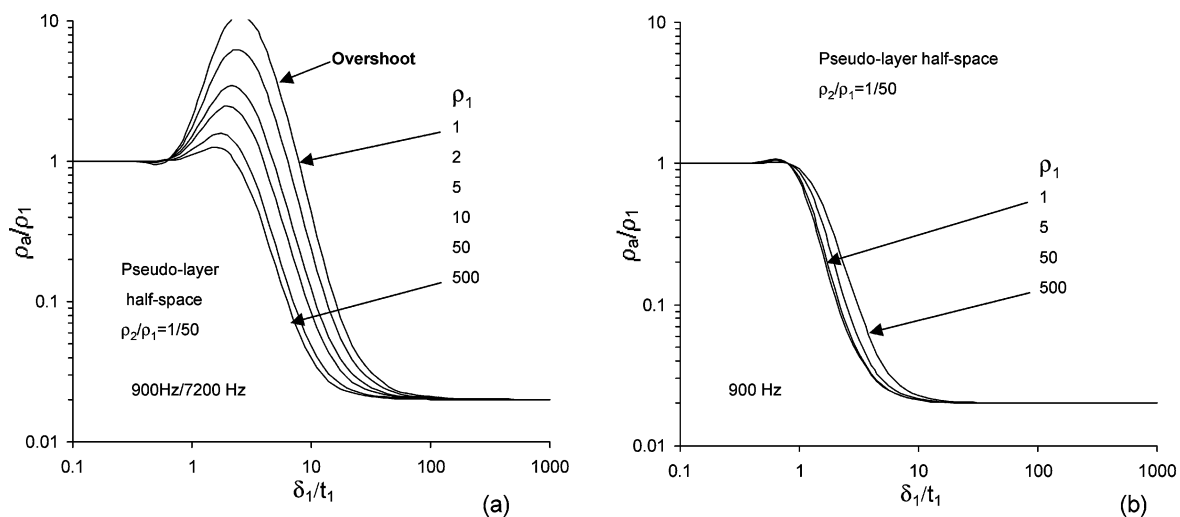

FIG. 4. (a) The 900/7200 Hz quad–quad resistivity of transform 12 and (b) the in-phase–quad resistivity of transform 1 for a suite of two-layer cases where the resistivities of the upper layer vary from 1 to 500 ohm-m and $\rho_2/\rho_1 = 1/50$. See Figure 2 for the abscissa and ordinate.

As with the other examples, the overshoot in Figure 5a (for a conductive lower layer) is larger than the undershoot (for a conductive upper layer) for equal resistivity contrast.

The frequency ratios f_H/f_L in the above examples are about 8. The influence of different frequency ratios for a fixed lower frequency is shown in Figure 5b. The amplitudes of the overshoot and undershoot of this quad–quad resistivity are fairly independent of the frequency ratio, although the response is shifted and spread along the abscissa, depending on this ratio.

Our modeling shows that the amount of overshoot and undershoot of the quad–quad resistivity for nonmagnetic two-layer cases depends mainly upon both the ratio of the lower frequency to the resistivity of the upper layer and the resistivity contrast, and slightly upon the frequency ratio.

The amount of overshoot or undershoot is also related to the skin depth of the lower frequency. This is to be expected since the skin depth in the upper layer is proportional to $\sqrt{(\rho_1/f_L)}$. For a two-layer case, a resistivity overshoot or undershoot tends to occur when the skin depth is about 1.5 to 2.5 times deeper than the two-layer interface for the upper-layer resistivity ρ_1

at the lower frequency f_L. For single-frequency analysis using the in-phase–quad algorithm, apparent resistivity may also overshoot or undershoot for an interface at this same depth. However, in-phase–quad resistivities only overshoot or undershoot the upper-layer resistivity by a few percent of the true resistivity. Therefore, this phenomenon is unimportant in practice when using the in-phase–quad algorithm.

Magnetic two-layer cases

We now show how quad–quad resistivity behaves for magnetic two-layer cases. Figure 6 presents the apparent resistivities for a suite of two-layer cases where the permeability is uniform for the two layers. Such a case simulates conductive or resistive cover over bedrock where the cover was produced by weathering or erosion that did not alter, attenuate, or concentrate the magnetite.

In generating the two panels of Figure 6, the forward solutions yield the in-phase and quadrature responses for the various frequencies. The permeability is computed from the
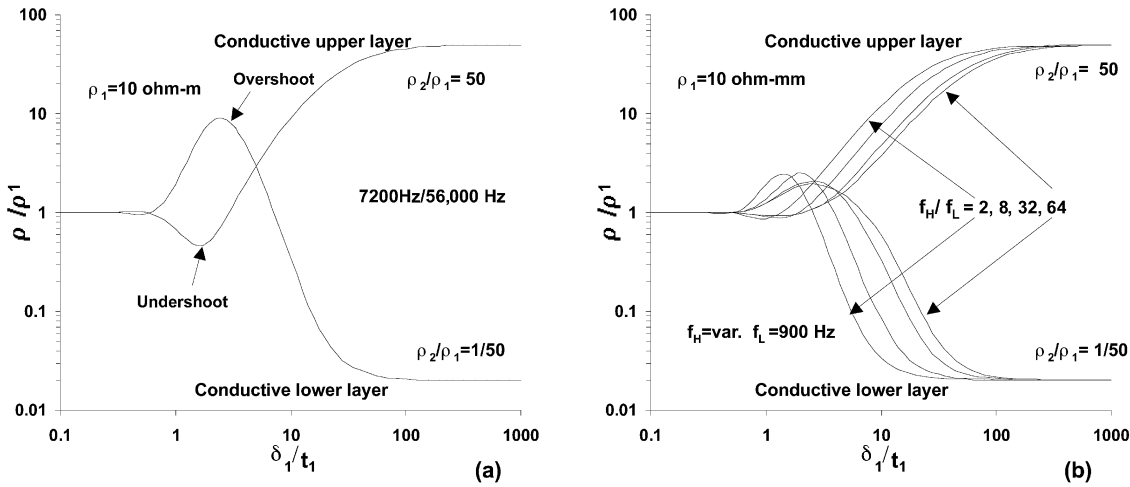

FIG. 5. (a) The 7200/56 000 Hz quad–quad resistivity of transform 12 for a suite of two-layer cases with an upper-layer resistivity of 10 ohm-m and with $\rho_2/\rho_1 = 50$ and 1/50. (b) The quad–quad resistivity curves for several ratios f_H/f_L of the high to low frequencies.
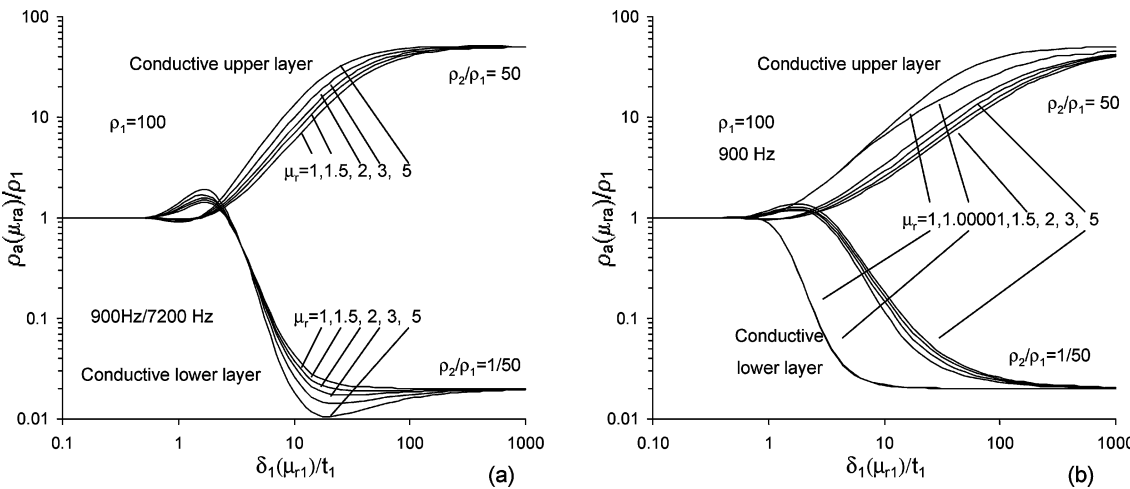

FIG. 6. The apparent resistivity curves for several relative magnetic permeabilities μ_r are obtained using (a) the quad–quad transform 14 for 900/7200 Hz and (b) the in-phase–quad transform 6 for 900 Hz. There is no permeability contrast between the magnetic layers.

900-Hz EM data (Huang and Fraser, 2000), and it is then used along with the in-phase and/or quadrature responses to obtain the apparent resistivity using the quad–quad (Figure 6a) and in-phase–quad (Figure 6b) algorithms. This approach yields virtually the correct input permeability as shown by Huang and Fraser (2000) when there is no permeability contrast between the layers.

The resistivity curves of Figure 6 illustrate that the apparent resistivities are impacted by the relative magnetic permeability μ_r. The in-phase–quad resistivity curves for the conductive upper-layer case of Figure 6b may seem strange, with the curve for $\mu_r = 5$ lying between those for $\mu_r = 1$ and $\mu_r = 1.5$. We have added the curve for $\mu_r = 1.00001$ to illustrate that even a vanishingly small permeability can have some impact on the response when the upper layer is conductive.

Figure 6 shows that the magnetic conductive half-space transforms yield permeability-dependent values for the apparent resistivities even when the correct permeability is used in the transformation to the half-space model. We use the expression nonpermeable apparent resistivity to refer to the apparent resistivity that is obtained for the nonmagnetic case of $\mu_r = 1$. When $\mu_r > 1$, an apparent resistivity that is identical to the nonpermeable apparent resistivity cannot be obtained through the transformation process when using half-space models, although it can be close to it under certain circumstances.

The deviation of the apparent resistivity curves for $\mu_r > 1$ from the nonpermeable apparent resistivity curves ($\mu_r = 1$) is more acute for the in-phase–quad algorithm (Figure 6b) than for the quad–quad algorithm (Figure 6a). The deviation of the quad–quad resistivity is generally not serious when the relative magnetic permeability is less than 2, i.e., when the amount of magnetite is less than about 20% by volume. Magnetic rocks seldom contain this much magnetite, apart from the iron formations. Thus, there is a strong reason for using the quad–quad algorithm in magnetic terrain notwithstanding the danger of resistivity overshoot and undershoot that can occur, e.g., at about $\delta_1/t_1 = 2$ in Figure 6a. In this figure, the amount of overshoot or undershoot in the apparent resistivity increases only slightly with magnetic permeability.

In our testing of magnetic-resistivity half-space transformation methods, we also varied the permeability between the layers, which of course led to many more combinations of parameters. The testing of such cases yielded results similar to those of Figure 6.

Deviation of apparent resistivities from nonpermeable apparent resistivity

The expression nonpermeable apparent resistivity was used above to refer to the apparent resistivity obtained from half-space models having a relative magnetic permeability μ_r of 1. We showed that the effect of a permeability $\mu_r > 1$ tends to yield an apparent resistivity for a layered earth which differs from the nonpermeable apparent resistivity obtained from the same resistivity layering but with $\mu_r = 1$.

A means of quickly observing the effect of permeability on the half-space transformation of layered-earth data is to perform two operation. First, compute the apparent resistivity curves for various values of relative magnetic permeability as shown, for example, in Figure 6. Second, divide the apparent resistivity values for $\mu_r > 1$ by the apparent resistivity values

for $\mu_r = 1$ for that layered-earth case. If the apparent resistivity ratio for $\mu_r > 1$ is unity, then the apparent resistivity for $\mu_r > 1$ is equal to that for $\mu_r = 1$ and so the permeability does not affect the apparent resistivity. If not equal to unity, the apparent resistivity differs from the nonpermeable apparent resistivity.

Figure 7 presents a plot of the apparent resistivity ratio for magnetic two-layer cases with resistivity contrasts of 50 and 1/50. Both layers have the same permeability. The deviations of the apparent resistivity ratios from unity are immediately seen and quantified. Figures 7a and 7b show the resistivity deviations for the quad–quad algorithm for 900/7200 Hz, and Figures 7c and 7d show the deviations for the in-phase–quad algorithm for 900 Hz. The deviations of the apparent resistivity from the nonpermeable apparent resistivity are greater for the in-phase–quad algorithm. The deviations are much less severe for the quad–quad algorithm—particularly for those permeabilities likely to be encountered in nature, i.e., when $\mu_r < 2$. The type of plot shown in Figure 7 is helpful in quickly assessing whether the in-phase–quad algorithm or the quad–quad algorithm would be more useful for resistivity mapping in a given survey area.

When to use and when to avoid the quad–quad algorithm

We have shown that apparent resistivity computed from the quad–quad algorithm is much less sensitive to magnetic polarization currents than is the in-phase–quad algorithm. This bodes well for using the quad–quad algorithm for resistivity mapping in magnetic terrains. However, we have also shown that the quad–quad algorithm can give a misleading picture with severe undershoots or overshoots. For multifrequency electrical sounding, the quad–quad algorithm has the disadvantage of yielding one less apparent resistivity value since it requires data from two frequencies compared to the single frequency of the in-phase–quad algorithm. A further disadvantage is that the sensitivity of the apparent resistivities to buried conductors is less for the quad–quad algorithm when the terrain is nonmagnetic.

The in-phase–quad algorithm should always be preferred in the absence of significant magnetic permeability. In magnetic terrain, the quad–quad algorithm is preferable but should be used with care to avoid misinterpretation caused by a misleading apparent resistivity presentation arising from high induction numbers. Generally speaking, the quad–quad algorithm should not be used if $f_L/\rho_1 > 500$ Hz/ohm-m in areas where conductive overburden exists and if $f_L/\rho_1 > 50$ Hz/ohm-m in areas where a conductive basement underlies resistive cover.

A FIELD EXAMPLE

A field example using Dighem survey data is presented in Huang and Fraser (2000). The survey is from an area in southern Africa where the strata are gently dipping and highly magnetized in places and where the overburden is conductive with a variable thickness. Figures 9 and 10 in Huang and Fraser (2000) compare the quad–quad resistivity with the in-phase–quad resistivity for several frequencies and also compares the EM-derived magnetic susceptibility with the total field magnetic data.

We show one example from this field data to illustrate that the quad–quad resistivity is fairly independent of the input permeability. Figures 8a and 8b, respectively, present the

quad–quad resistivity where (a) the input permeability is free space and (b) the input permeability was first computed from the EM data, where the magnetic susceptibilities ranged from 0 to 170×10^{-3} SI units (up to 5% magnetite). The two figures visually are almost identical, illustrating that the output quad–quad resistivity is quite forgiving of errors in the input magnetic permeability. This is to be expected from our testing of the quad–quad algorithm. On the other hand, the output in-phase–quad resistivity is not forgiving of errors in the input permeability, as shown in Huang and Fraser (2000). Therefore, if the magnetic permeability has not been obtained from the EM data or is suspect, the quad–quad algorithm should be used to compute the apparent resistivity.

CONCLUSIONS

The behavior of the quad–quad (apparent) resistivity in comparison to the in-phase–quad resistivity has been studied to determine the conditions under which quad–quad resistivity can be useful. If the ratio of the lower frequency f_L to the upper-layer resistivity ρ_1 is low (see below), the quad–quad resistivity will behave well. In areas yielding a high value of f_L/ρ_1, the quad–quad resistivity may lie outside of the range of the true resistivities and therefore provide misleading information. These problems are exacerbated when large resistivity contrasts exist (e.g., ρ_2/ρ_1 for a two-layer earth). This indicates the quad–

quad resistivity algorithm should be avoided when using high frequencies in conductive areas. This often is not a serious limitation, bearing in mind that the primary use of the quad–quad resistivity algorithm is in highly magnetized areas. Such terrains often appear to be fairly resistive; otherwise, magnetic polarization currents are usually not sensed by the EM system.
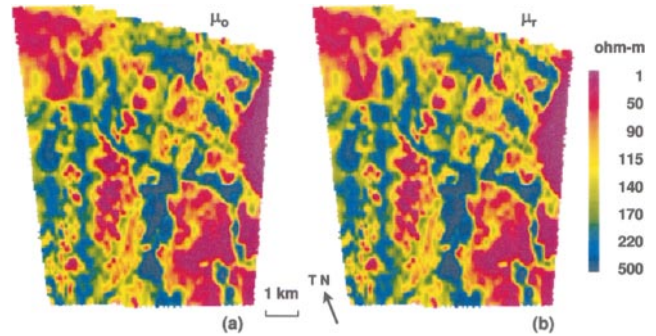

FIG. 8. Quad–quad resistivity maps for 400/7200 Hz are shown (a) using transform 12 with an input magnetic permeability of free space and (b) using transform 14 with the input (precomputed) apparent permeability being taken from Figure 9b of Huang and Fraser (2000).
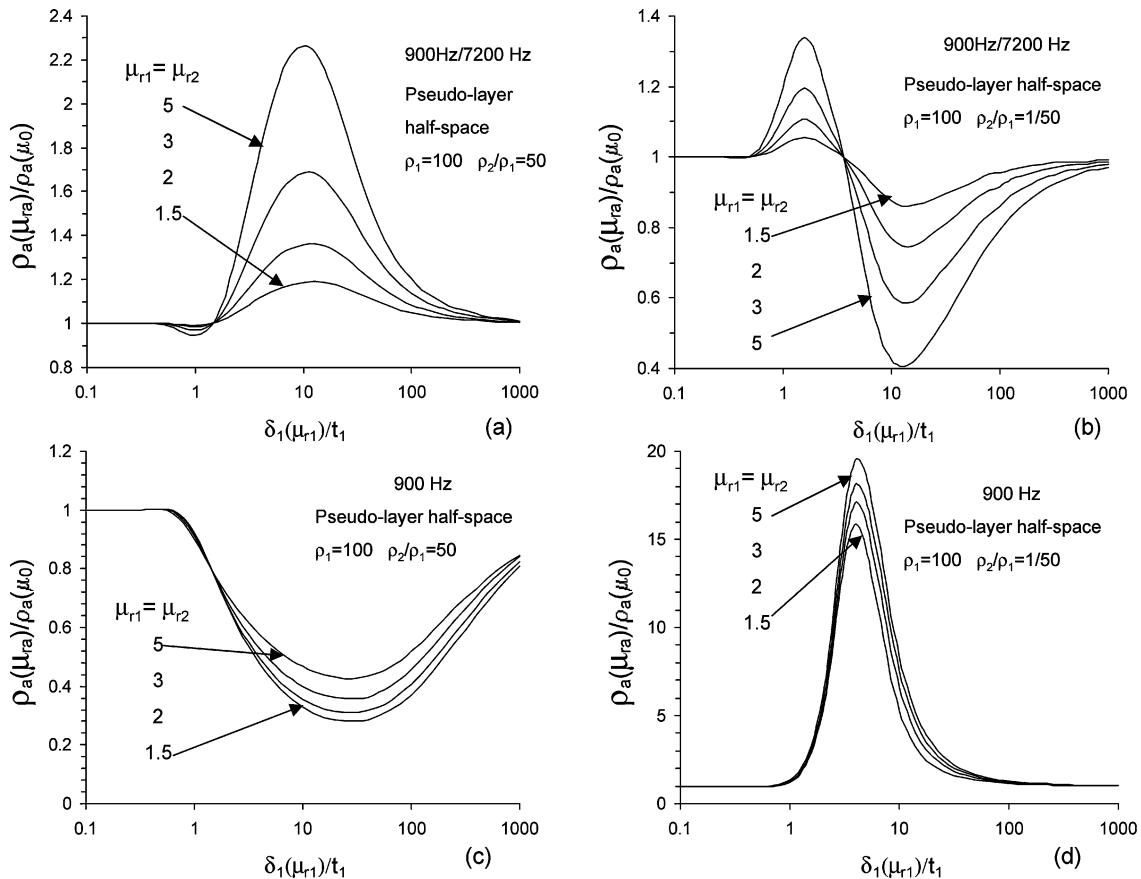

FIG. 7. The deviations of the quad–quad resistivity of transform 14 for 900/7200 Hz from the nonpermeable apparent resistivity are shown for four different relative magnetic permeabilities μ_r for two-layer cases with resistivity contrasts of (a) 50 and (b) 1/50. The deviations for the in-phase–quad resistivity of transform 6 are shown for the same two-layer cases with resistivity contrasts of (c) 50 and (d) 1/50. There is no permeability contrast between the magnetic layers. Note the differences in the ordinate scales.

Where thick conductive cover exists over highly magnetic rocks, there will be little evidence of magnetic polarization currents because the conduction currents in the cover will dominate. In such a case, there is no incentive to use the quad–quad resistivity algorithm. Quad–quad resistivity is recommended only when $f_L/\rho_1 < 500$ Hz/ohm-m in magnetic areas where conductive overburden exists and when $f_L/\rho_1 < 50$ Hz/ohm-m in magnetic areas where a conductive basement underlies a resistive cover. In very conductive areas or in the absence of significant magnetic permeability, the in-phase–quad algorithm is always preferable. Apart from these situations, the quad–quad resistivity algorithm often yields superior results in magnetic areas.

ACKNOWLEDGMENTS

REFERENCES

Fraser, D. C., 1978, Resistivity mapping with an airborne multicoil electromagnetic system: Geophysics, **43**, 144–172.
——— 1990, Layered-earth resistivity mapping, *in* Fitterman, D. V., Ed., Developments and applications of modern airborne electromagnetic surveys: U. S. Geol. Surv. Bull. **1925**, 33–41.
Huang, H., and Fraser, D. C., 1996, The differential parameter method for multifrequency airborne resistivity mapping: Geophysics, **61**, 100–109.
——— 1998, Magnetic permeability and electrical resistivity mapping with a multifrequency airborne EM system: Expl. Geophys., **29**, 249–253.
——— 2000, Airborne resistivity and susceptibility mapping in magnetically polarizable areas: Geophysics, **65**, 502–511.
——— 2001, Mapping of the resistivity, susceptibility, and permittivity of the earth using a helicopter-borne electromagnetic system: Geophysics, **66**, 148–157.
——— 2002, Dielectric permittivity and resistivity mapping using high-frequency helicopter-borne EM data: Geophysics, **67**, in press.
Morrison, H. F., Phillips, R. J., and O'Brien, D. P., 1969, Quantitative interpretation of transient electromagnetic fields over a layered half-space: Geophys. Prosp., **17**, 82–101.
Sengpiel, K. P., 1988, Approximate inversion of airborne EM data from a multilayered ground: Geophys. Prosp., **36**, 446–459.
Sengpiel, K. P., and Siemon, B., 2000, Advanced inversion methods for airborne electromagnetic exploration: Geophysics, **65**, 1983–1992.
Spies, B. R., and Eggers, D. E., 1986, The use and misuse of apparent resistivity in electromagnetic methods: Geophysics, **51**, 1462–1471.